Evolution, 55(11), 2001, pp. 2181–2193

FROM METABOLISM TO POLYMORPHISM IN BACTERIAL POPULATIONS: A THEORETICAL STUDY

EMMANUELLE PORCHER,[1,2] OLIVIER TENAILLON,[3,4] AND BERNARD GODELLE[5,6]
[1]*Laboratoire Ecologie, Systématique et Evolution, Université Paris-XI/CNRS UPRES-A 8079, Bâtiment 362, 91405 Orsay cedex, France*
[2]*E-mail: Emmanuelle.Porcher@esv.u-psud.fr*
[3]*Génétique Moléculaire Evolutive et Médicale, E9916 INSERM, Faculté de Médecine Necker-Enfants Malades, Université René Descartes-Paris V, 156 Rue de Vaugirard, 75730 Paris cedex 15, France*
[4]*E-mail: tenaillon@necker.fr*
[5]*Laboratoire Génome, Populations, Interactions, UMR 5000, Université Montpellier II, place Eugène Bataillon, 34095 Montpellier cedex 5, France*
[6]*E-mail: godelle@crit.univ-montp2.fr*

Abstract.—Stable polymorphisms are commonly observed in experimental bacterial populations grown in homogeneous media. Evidence is accumulating that metabolic interactions might be the main mechanism underlying the emergence and maintenance of such polymorphisms. To date, however, attempts to model the evolution of bacterial polymorphism have not considered metabolism as a possible component of polymorphism maintenance. Here, we propose a simulation approach to model the evolution of selected polymorphisms in a bacterial population. Using recent knowledge of the relationship between bacterial fitness and metabolism, we build a simple metabolic model and test the effect of resource competition on polymorphism. Without making an a priori hypothesis on fitness functions, we show that stable polymorphic situations could be observed under high nutrient competition, and we propose a functional, metabolism-based explanation to the debated issue of polymorphism maintenance.

Key words.—Bacteria, biodiversity, competitive exclusion principle, model, nutrient competition.

Received January 25, 2001. Accepted July 16, 2001.

A large number of experimental studies have been performed to examine the evolution of genetic polymorphisms in bacterial populations. Some have revealed that selected polymorphisms may appear and be maintained in bacterial populations growing on a single resource (Levin 1972; Rosenzweig et al. 1994; Rainey and Travisano 1998; Rainey et al. 2000; Rozen and Lenski 2000). All of these studies showed that such stable polymorphisms are mostly attributable to frequency-dependent selection, acting through cross-feeding interactions (Levin 1972; Elena and Lenski 1997; Rainey and Travisano 1998; Treves et al. 1998). In other words, these selected genetic polymorphisms were supposed to be maintained through metabolic exchanges between the different genotypes. For example, Rosenzweig et al. (1994), by growing a single *Escherichia coli* clone in a glucose-limited medium, observed the emergence and maintenance of three phenotypically distinct clones differing in their pattern of secretion and uptake of two alternatives metabolites.

The maintenance of selected polymorphisms in bacterial populations has been the subject of few theoretical studies (Levin 1972; Stewart and Levin 1973), with none of them accounting for the apparently major and widespread role of metabolic interactions. These authors instead referred to classical mechanisms acting at the population level. For example, Stewart and Levin (1973) showed that two bacterial species could coexist on a single resource if the availability of the resource varied with time and if the relationship between growth rate and resource concentration differed between the two species. Subsequently, various frequency-dependent mechanisms, such as phage-mediated selection or allelopathy, were proposed as explanations of the observed genotypic frequencies in natural bacterial populations (Levin 1988).

One of the reasons why metabolism has been neglected in models of polymorphism maintenance could be the difficulty in finding a relationship between fitness and the complex metabolism of an organism. However, evidence is accumulating that the metabolism of a bacteria is a major component of fitness (Dean et al. 1986; Dykhuizen and Dean 1990), and simple relationships between fitness and enzyme activities on a major pathway have been observed experimentally. Dykhuizen and Dean (1990), for example, in trying to assess a causal relationship between genotype and fitness, showed that fitness is strictly proportional to the metabolic flux through the lactose pathway of *E. coli* cells grown in a chemostat.

In this paper, we aim to explain the emergence, evolution, and maintenance of bacterial polymorphisms in terms of metabolic interactions, using knowledge of components of fitness in bacteria (Dykhuizen and Dean 1990). Previous theoretical studies were based on mathematical fitness functions, with assumptions on the way fitness changed with the environment. Here, we use a simple metabolic model and simulate the evolution of a bacterial population exposed to a new environment. We demonstrate that such a mechanistic model can describe realistically the evolution and polymorphism of empirically studied bacterial populations. Thus, we propose a functional explanation for the maintenance of selected polymorphisms in bacterial populations.

THE MODEL

We simulate the evolution of an asexual bacterial population experiencing a novel environment, a situation sometimes encountered by soil bacteria submitted to pollution and that resembles the culture conditions in the experiments by Levin (1972), Elena and Lenski (1997), Rainey and Travisano

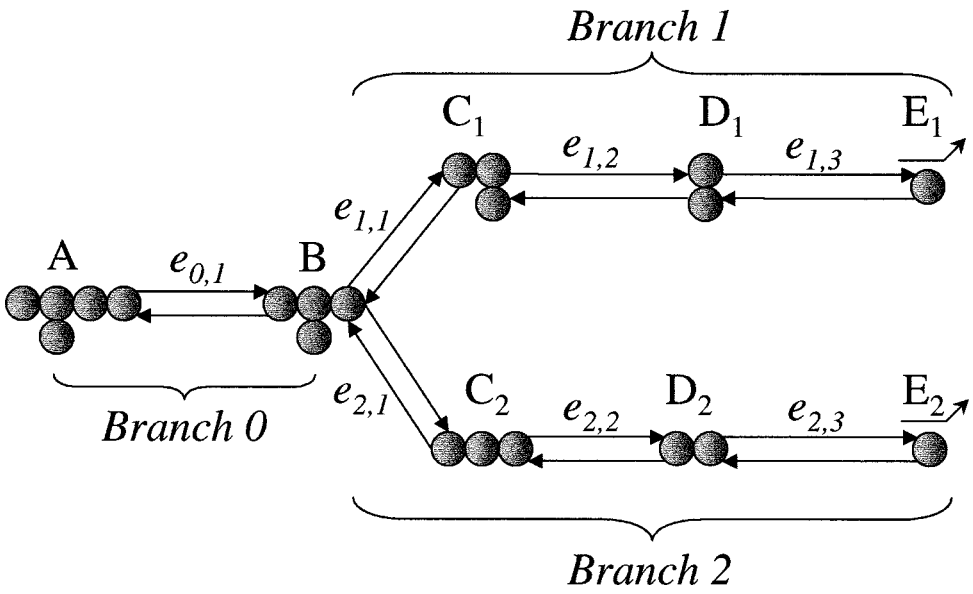

FIG. 1. The metabolic pathway. *A* is an organic compound whose concentration is maintained at a constant value (=100 μM) in the cytoplasm. Its degradation follows two different branches in the pathway. Each reaction *j* in branch *i* is reversible, exergonic, and catalyzed by an enzyme, $E_{i,j}$ with activity $e_{i,j}$. The final products of the pathway, E_1 and E_2, do not remain in the system.

(1998), and Treves et al. (1998). This environment is characterized by a constant influx of a single biodegradable organic compound *A,* for example, a xenobiotic (Alexander 1981; Leahy and Colwell 1990; Macaskie et al. 1997; Lee et al. 1998). We assume that bacteria can degrade *A* using a branched pathway (Fig. 1), a widespread pattern in bacterial metabolism (Hastings 1992); each reaction of this pathway produces one ATP molecule. The enzymatic activities on the branched pathway are modifiable by mutations. We use metabolic control theory (Kacser and Beeby 1984; Keightley and Kacser 1987) to calculate the energy production of a cell as a function of its enzymatic activities. Using data from the literature, the speed of division of the cells is derived from the energy production.

Analytical Approach: Energy Production of an Isolated Cell

Metabolic control theory (Kacser and Beeby 1984; Keightley and Kacser 1987) describes the relation between enzyme activities and metabolism. We use results of this theory to calculate the metabolic fluxes (i.e., the velocities of metabolic reactions) in the branched pathway (Fig. 1). The levels of metabolic fluxes are then used to calculate the energy production of the bacteria.

Definitions

Enzyme activity is usually defined as the ratio of the maximum velocity of an enzyme ($V_{\max}$) on its half-saturation constant (K_M). Each reaction, *i*, of the pathway is characterized by the substrate, S_i, and product, S_{i+1}, of the reaction, its thermodynamic equilibrium constant, Ke_i, and the activity of its catalyzing enzyme, e_i ($= V_{\max_i}/K_{M_i}$). When the enzyme is unsaturated, i.e., when the concentration $[S_i]$ of its substrate S_i is low relative to its half-saturation constant, K_M, the velocity of reaction *i* (v_i) is given by a simplified Briggs-Haldane equation:

$$v_i = e_i([S_i] - [S_{i+1}]/Ke_i). \quad (1)$$

Metabolic fluxes at steady state

The steady state of a metabolic system is defined by constant velocities of all reactions and constant metabolite concentrations. This implies that velocities are the same for all the reactions within a branch of a pathway and equal the velocity in the whole branch. In the branched pathway of the model (Fig. 1), the fluxes (or velocities) J_0, J_1, and J_2 in the three branches are such that: $J_0 = J_1 + J_2$. At steady state:

$$J_0 = v_0 = e_{0,1}\{[A] - [B]/K_{0,1}\}, \quad (2a)$$

$$\begin{aligned} J_1 = v_{1,1} = v_{1,2} = v_{1,3} &= e_{1,1}\{[B] - [C_1]/K_{1,1}\} \\ &= e_{1,2}\{[C_1] - [D_1]/K_{1,2}\} \\ &= e_{1,3}\{[D_1] - [E_1]/K_{1,3}\}, \quad \text{and} \end{aligned} \quad (2b)$$

$$\begin{aligned} J_2 = v_{2,1} = v_{2,2} = v_{2,3} &= e_{2,1}\{[B] - [C_2]/K_{2,1}\} \\ &= e_{2,2}\{[C_2] - [D_2]/K_{2,2}\} \\ &= e_{2,3}\{[D_2] - [E_2]/K_{2,3}\}, \end{aligned} \quad (2c)$$

$K_{i,j}$ is the equilibrium constant of the *j*th reaction in branch *i* (containing *n* reactions) and $e_{i,j}$ is the activity of the enzyme catalyzing the *j*th reaction in branch *i*. We assume that the intracellular concentration of *A* is constant (see Algorithm: Metabolic equilibration) and that the final products of the branched pathway do not accumulate in the population: $[E_i] = 0$ (i.e., they were either gases or metabolic compounds used very rapidly in another pathway). Given these assumptions, after some rearrangements, the set of equations listed above yields:

$$J_0 = \frac{1}{a_0}\left([A] - \frac{[B]_{SS}}{K_{0,1}}\right), \quad (3a)$$

$$J_1 = \frac{[B]_{SS}}{a_1}, \quad (3b)$$

$$J_2 = \frac{[B]_{SS}}{a_2}, \quad (3c)$$

$$a_0 = 1/e_{0,1}, \quad (3d)$$

$$a_1 = 1/e_{1,1} + 1/(e_{1,2}K_{1,1}) + 1/(e_{1,3}K_{1,2}K_{1,1}), \quad (3e)$$

$$a_2 = 1/e_{2,1} + 1/(e_{2,2}K_{2,1}) + 1/(e_{2,3}K_{2,2}K_{2,1}), \quad \text{and} \quad (3f)$$

$$[B]_{SS} = [A]a_1a_2/\{a_0a_1 + a_0a_2 + a_1a_2/K_{0,1}\}, \quad (3g)$$

where $[B]_{SS}$ is the steady-state concentration of metabolite *B*. We set all $K_{i,j}$ at the constant value of 10, which means that each forward reaction is highly exergonic. Steady-state concentrations of other metabolites can also be derived from these equations (see Appendix).

Energy production

One ATP molecule being produced by each reaction, the flux, *E*, of energy produced by the pathway can thus be written as a simple function of metabolic fluxes in the three branches:

$$E = J_0 + 3J_1 + 3J_2. \quad (4)$$

This metabolic model, allowing the calculation of energy production in an isolated cell, is then used as a basis to simulate the growth and evolution of a bacterial population consisting of permeable cells, exchanging metabolites.

Algorithm of the Model

Limits of the steady-state hypothesis

The steady-state hypothesis is useful in metabolic models because it provides analytic results in terms of metabolic fluxes within an isolated cell. However, if one is to take metabolic exchanges between several genotypes into account, the problem rapidly becomes intractable because the number of equations to be solved increases with the number of coexisting genotypes. Thus, a steady state at the population level cannot be calculated in our model, due to a possibly high level of polymorphism in the metabolic pathway. To solve this problem, we run simulations where metabolic exchanges are uncoupled from catalytic reactions and two phases are distinguished: (1) An equilibration phase, during which the cells actively exchange metabolites with their environment; and (2) a catalytic phase, during which the bacterial membranes are closed, reactions occur, and the cellular metabolism can reach steady state. During this catalytic phase, the basic metabolic model is used to calculate the energy production of the isolated cells. The equilibration phase is considered instantaneous. The duration of the catalytic phase, Δt, is constant within a simulation and is chosen never to exceed 20 min, the generation time of *E. coli* under ideal laboratory conditions.

Algorithm

The computation of the evolution of the population from generation t to generation $t + 1$ consists of five main phases: equilibration, division, mortality, mutation, and random sampling (Fig. 2). The population is divided into G genotypes defined by their activities on the seven enzymes of the metabolic pathway. Genotypes are named from these enzymatic activities, and n_g is the number of cells having the same genotype g (clones). The five phases are described below.

Metabolic equilibration.—During the equilibration phase, the cells are considered permeable, which means that metabolic exchanges occur between the cells and their environment. We assume an active transport of metabolites across the bacterial membranes. Given the observed ability of bacteria to maintain high concentrations for key nutrients (Ferenci 1996; Prescott et al. 1996), we impose the following characteristics on these transports: (1) the intracellular concentration of *A* ($[A]_i$) remains constant during a whole simulation, whatever the extracellular concentration; and (2) after the equilibration phase, the intracellular concentrations of the other compounds ($[X]_i$) are 10 times higher than their extracellular concentrations for all genotypes: $[X]_i(t) = 10[X]_e(t)$. The energetic requirement of these active transports is not taken into account; we assume it identical for all the cells and include it into a basal metabolism. Given these characteristics for metabolic transports, the intracellular and environmental concentrations of each metabolite *X*, $[X]_i(t)$ and $[X]_e(t)$, are calculated, knowing both the intracellular steady state concentrations $[X]_{SSg}(t - 1)$ of each genotype g and the environmental concentrations $[X]_e(t - 1)$ at generation $t - 1$, before equilibration. The total quantity of metabolites being constant during equilibration,

$$\sum_g \{n_g[X]_{SSg}(t - 1)v\} + [X]_e(t - 1)V = \sum_g \{n_g[X]_i(t)v\} + [X]_e(t)V. \quad (5)$$

Because $[X]_i(t) = 10[X]_e(t)$, this yields:

$$[X]_e(t) = \frac{\left\{\sum_g [n_g[X]_{SSg}(t - 1)v] + [X]_e(t - 1)V\right\}}{\left[10\sum_g (n_g v) + V\right]}, \quad (6)$$

where v is the volume of a bacterial cell (2.25×10^{-18} m^3; Prescott et al. 1996) and V is the volume of the environment (10^{-6} m^3). These calculations are not applied to *A*, whose intracellular concentration remains constant.

Catalytic phase: energy production and division.—After equilibration, the cells are considered isolated. The basic metabolic model is used to calculate energy production at steady state, but some energy is also produced before the intracellular concentrations reach steady state. Reactions that occur in the beginning of catalytic phase lead the intracellular concentrations to steady state concentrations (Fig. 3). For each metabolite *X*, the amount of energy produced on this way to steady state is proportional to $([X]_i - [X]_{SS})$, one ATP molecule being produced for each transformed metabolite molecule. Steady state is reached more or less rapidly depending

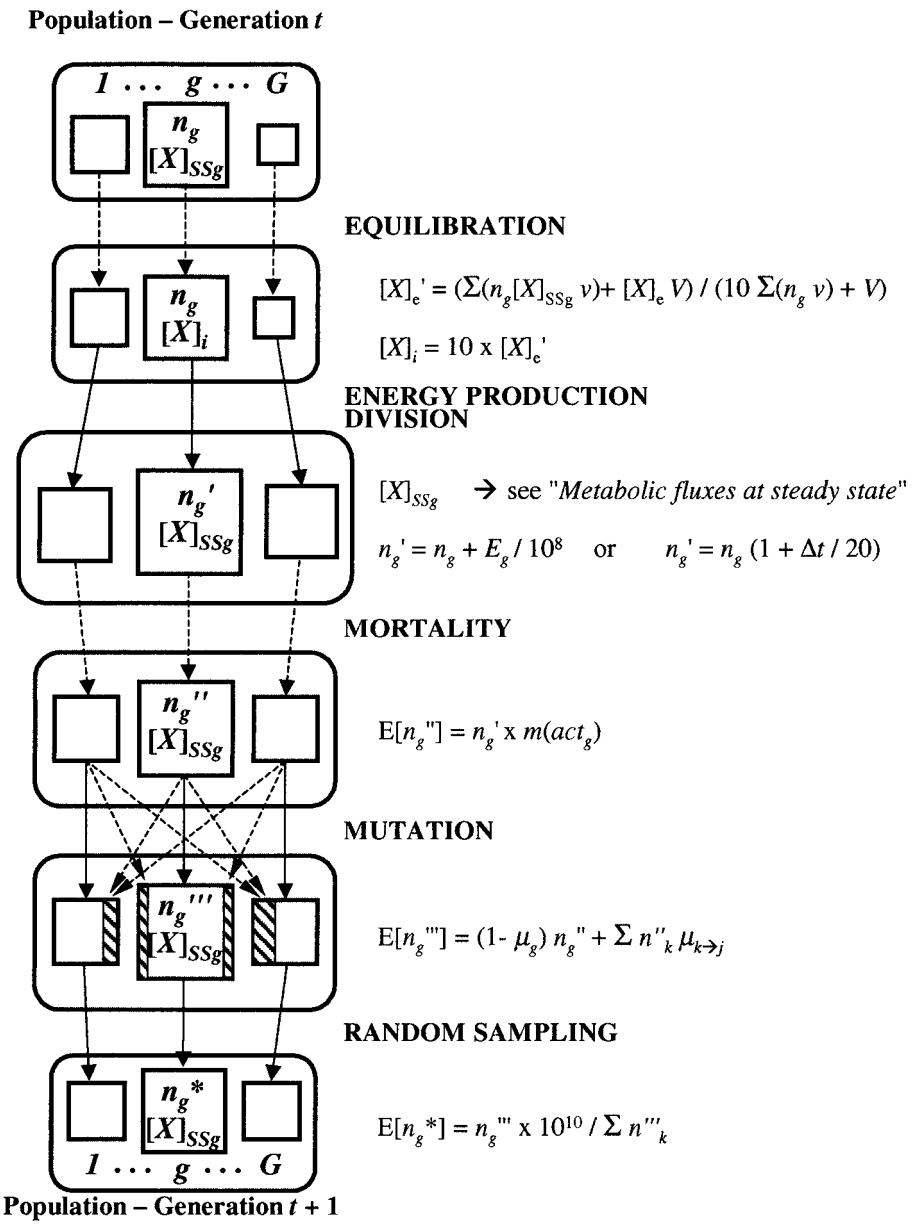

FIG. 2. Description of the algorithm used in the simulation models. See discussion in the text. This figure is modified from Tenaillon et al. (1999).

on enzymatic activities of the cell (Fig. 3). In efficient genotypes, steady state is reached within 1 min, and more energy is produced through a constant flux. Genotypes with poor efficiency, on the contrary, do not reach steady state within Δt, the duration of catalytic phase.

Thus, the energy production of a genotype g is

$$E_g = n_g\left[\sum_X ([X]_i - [X]_{SSg})v + (J_0 + 3J_1 + 3J_2)\Delta t\right] \quad (7)$$

(if steady state is reached very quickly within Δt) or

$$E_g = n_g\left(\sum_X [X]_i - [X]_{\Delta t}\right)v, \quad (8)$$

where J_i is the flux in branch i of the metabolic pathway and $[X]_{\Delta t}$ the intracellular concentration of metabolite X at the end of the catalytic phase in cells with poor efficiency.

However, the influx of A (J_A) is not always sufficient to sustain the energy production of all the cells, depending on population size or enzymatic activities of the genotypes. Bacteria can thus undergo nutrient competition when the influx of A (J_A) in the environment is not sufficient to sustain the growth of the whole population. To model this nutrient competition, we calculate the global requirement of the population for A,

$$J_{Areq} = \sum_g \left[n_g J_{0(g)} + \sum_X ([X]_i - [X]_{SSg})\right] \quad (9)$$

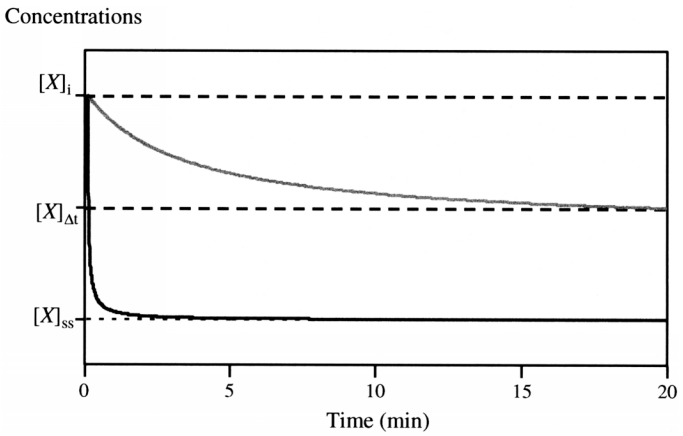

FIG. 3. Schematic representation of the change in concentration of metabolite X during catalytic phase. The concentration of one of the metabolites of the branched pathway was schematically plotted against time, in two enzymatic contexts. At the beginning of catalytic phase ($t = 0$), the initial concentration ($[X]_i$) was different from the steady state concentration, $[X]_{SS}$, and the change in concentration of the metabolite was followed when the system reached steady state. The energy production of the cell was proportional to the amount of metabolite consumed during this phase. The enzymatic contexts were the following: (1) highly efficient cell (black line); the activities of the first enzymes of the metabolic pathway exceeded 1 min^{-1}; the steady state concentration ($[X]_{SS}$) was reached within 1 min; the flux through the metabolic pathway was constant afterward; and (2) poorly efficient cell (gray line); the activities of the first enzymes of the metabolic pathway were smaller than 0.1 min^{-1}; the concentration after Δt($[X]_{\Delta t}$) was far from steady state concentration; no constant flux was established within the cell.

and compare it to J_A. When $J_{Areq} > J_A$, the influx of A is limiting, and the flux through the metabolic pathway is decreased by the factor J_A/J_{Areq} in all the cells, whatever the enzyme activities, thus creating scramble competition. This yields, for energy production of efficient cells:

$$E_g = n_g\left\{\sum_X [([X]_i - [X]_{SSg})v] + (J_0 + 3J_1 + 3J_2)\Delta t(J_A/J_{Areq})\right\}. \quad (10)$$

The division of a bacterial cell requires a fixed amount of energy, allocated to protein synthesis, DNA replication and other metabolic functions (Senez 1962; Prescott et al. 1996). Division occurs when the energetic accumulation of a cell reaches this threshold. The relationship between energy production and speed of division is thus linear for low energy production, but it then reaches a plateau, the generation time cannot be smaller than 20 min, because DNA replication or protein synthesis might also depend on polymerases or ribosomes efficiencies (Fig. 4A), which could not evolve in our model. The amount of energy required for division is 10^8 ATP molecules (10^8–10^9, Senez 1962; Prescott et al. 1996). The new number of cells of genotype j is thus $n_g(t) = n_g(t - 1) + E_g(t)/10^8$ if division time ($= 10^8 \times \Delta t/E_g[t]$) > 20 min, and $n_g(t) = n_g(t - 1)\ (1 + \Delta t/20)$ otherwise. Energy used for division is removed from the energetic reserve of each genotype.

Mortality.—We choose a reference mortality rate of 10^{-2} per cell per generation, which corresponds to the mortality rate in soil bacterial populations, as estimated by Savageau (1983). We furthermore assume that mortality is dependent on enzymatic activity ($m[act]$, Fig. 4B) to limit the total enzymatic activity of a cell (i.e., the sum of the seven enzymatic activities): Because enzymatic activities depend on enzyme production, we assume that the total activity of a cell cannot exceed a threshold value. The overexpression of enzyme leads to cell death (Fig. 4B), as observed in *E. coli* (Koch 1983; Dong et al. 1995). This constraint effectively limits the number of efficient enzymes (i.e., enzymes whose activities are 10 min^{-1}) in the metabolic pathway. In the mortality process, individuals are randomly removed from each genotype to simulate death, according to basal death rate and activity-induced mortality, $m[act]$. The number of dead cells per genotype is drawn using Poisson distribution.

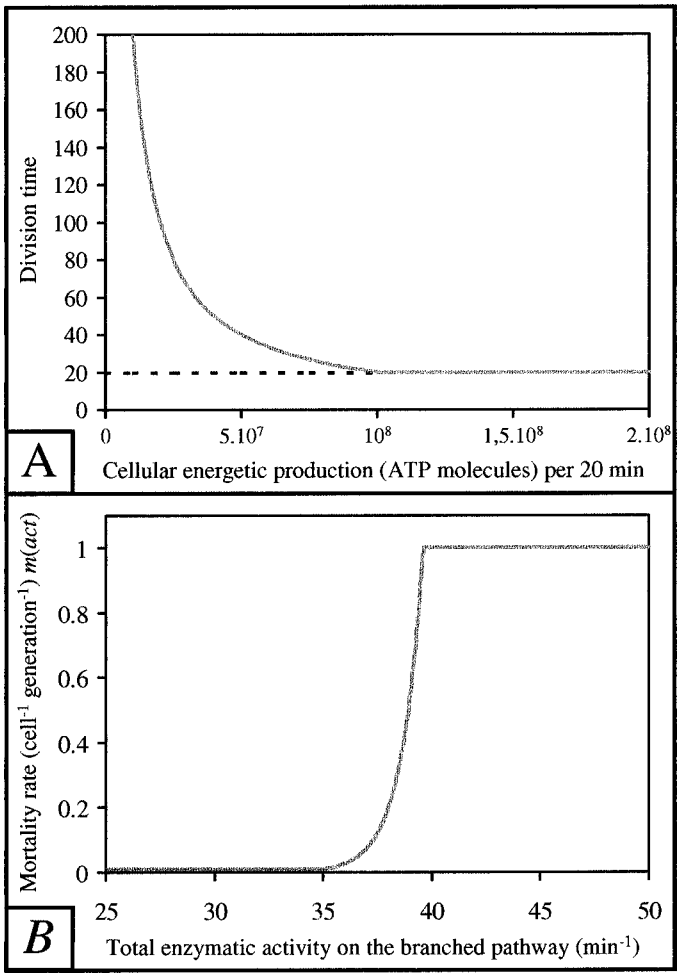

FIG. 4. Division time and mortality rate in a model cell. (A) Relationship between division time and energy production. The cellular energy production was measured as the number of energetic units produced by one cell during 20 min. (B) Cell mortality rate as a function of the total enzymatic activity on the branched pathway. In the model, the total enzymatic activity was the sum of the activities of the seven enzymes. Above a threshold value (35 min^{-1}), the mortality increased exponentially with the excess of activity ($m[act] = 0.01e^{[act-35]}$), up to a probability of one.

Mutation.—We assume that the reactions involved in the

TABLE 1. Mutation rates on the metabolic pathway.

Initial enzymatic activity (min^{-1})	Enzymatic activity of the mutant (min^{-1})			
	0.01	0.1	1	10
0.01	—	10^{-8}	10^{-9}	10^{-10}
0.1	10^{-8}	—	3×10^{-9}	3×10^{-10}
1	10^{-8}	10^{-8}	—	10^{-9}
10	10^{-8}	10^{-8}	10^{-8}	—

metabolism of *A* are at first catalyzed by nonspecific enzymes preexisting in the pool of bacterial proteins (>4200 for *E. coli*; Blattner et al. 1997). This means that the initial population contains only one genotype, with low activity for all the reactions. The genes coding for these seven enzymes can mutate, which may increase (or decrease) catalyzing activities. We assume discrete effects of mutation on the enzymatic activities. Activities can only take four values, ranging from 0.01 min^{-1} (nonspecific enzymes) to 10 min^{-1} (highly efficient catalysts), as observed for *E. coli* enzymes (Karp et al. 1999). The intermediate values are 0.1 min^{-1} and 1 min^{-1}. The basal mutation is 10^{-10} mutations per DNA base per generation, as estimated in Drake (1991). The mutation rates between levels of activity are chosen as follows: deleterious mutations, which decrease enzymatic activity, are relatively frequent (10^{-8}); the frequency of mutations increasing activity is negatively correlated with the magnitude of their effect (Table 1). We consider only single mutation events. During simulations, the number of mutants per genotype is randomly drawn using Poisson distributions, whose probabilities are given in Table 1.

Random sampling.—We assume a maximum capacity of the environment in terms of space availability. Initial population size is 10^9 and we let the population grow according to the bacterial metabolic capacities. Once the maximum capacity of the environment is reached, we keep the population size constant (10^{10}) by randomly removing supernumerary cells from the population. During the random sampling process, the size of the whole population is reduced to 10^{10} when necessary by randomly removing excess cells. Note that new genotypes can be generated by mutation and others can disappear due to random sampling process, so that the total number of genotypes varies during the simulation.

Genotype Nomenclature

To distinguish among genotypes, we assign each a seven-digit number. Each digit corresponds to an enzyme of the metabolic pathway (see Fig. 1: the first digit corresponds to enzyme $e_{0,1}$, etc.), and its value corresponds to the level of enzyme activity (levels 0, 1, 2, and 3 corresponds to the following enzyme activities respectively: 0.01, 0.1, 1, and 10 min^{-1}). For example, the genotype 3.210.000 produces enzyme $e_{0,1}$ at activity level 3 (10 min^{-1}), enzyme $e_{1,1}$ at activity level 2 (1 min^{-1}), enzyme $e_{1,2}$ at activity level 1 (0.1 min^{-1}), and enzymes $e_{1,3}$ and $e_{2,1}$ to $e_{2,3}$ at activity level 0 (0.01 min^{-1}).

Influence of Parameters

We test the effects of various parameters of the model, notably those for which we do not have any experimental estimates: (1) the intracellular concentration of *A*, $[A]_i$, the values of $[A]_i$ being 10, 100, and 1000 μM, which corresponds to realistic metabolic concentrations (Prescott et al. 1996); (2) the length of the catalytic phase Δt (5, 10, and 20 min); (3) the influx of *A* in the environment J_A (from 0.05 to 1 μM/20 min); and (4) the maximum total enzymatic activity of a cell (i.e., the threshold value above which death rate increases exponentially), which ranges from 25 to 70 min^{-1}, implying that a cell could possess from two to seven highly efficient enzymes. We also test the effects of parameters whose values are a priori better estimated: the basal death rate; the generation time; the equilibrium constants of the reactions, $K_{i,j}$; and the initial and maximum population size.

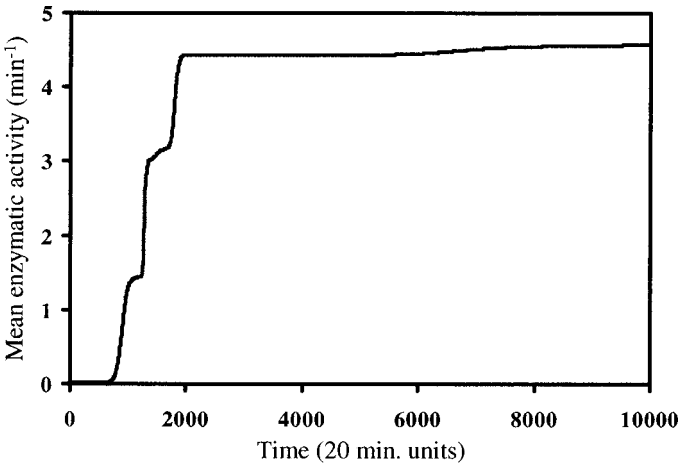

FIG. 5. Evolution of mean enzyme activity. One typical example (one simulation) of evolution is shown. The bacteria were subjected to the new environment at time 0, with mean enzymatic activity 0.01 min^{-1}. The parameters of the simulation were the following: influx of *A*, $J_A = 0.5$ μM/20 min (no resource competition), duration of the catalytic phase $\Delta t = 20$ min, intracellular concentration of *A*, $[A]_i = 100$ μM, maximum total enzymatic activity = 35 min^{-1}.

RESULTS

General Behavior of the Model

Mean enzyme activity showed a punctuated pattern of evolution (Fig. 5). Each jump corresponded to the replacement of a genotype by a fitter one (Fig. 6A). The major jumps corresponded to the fixation of highly efficient enzymes; their number (three in Fig. 5) was limited by overexpression-induced mortality. In most simulations, the population roughly needed 7000 units of time to reach maximum activity, which represents a period of about 3 months. The changes in genotypic composition of the population were correlated with changes in metabolic concentrations. For example, over a set of 15 simulations, this correlation, measured as the correlation between the inflexion times of one metabolic concentration and of the frequency of the invading genotype influencing this concentration (e.g., C_2 and 3.332.200 in Fig. 6) was strong ($r^2 = 0.9999$).

Several genotypes were often present in the population at the same time (Fig. 6A), but this polymorphism was transient and reflected a succession of genotypes, a mutant genotype

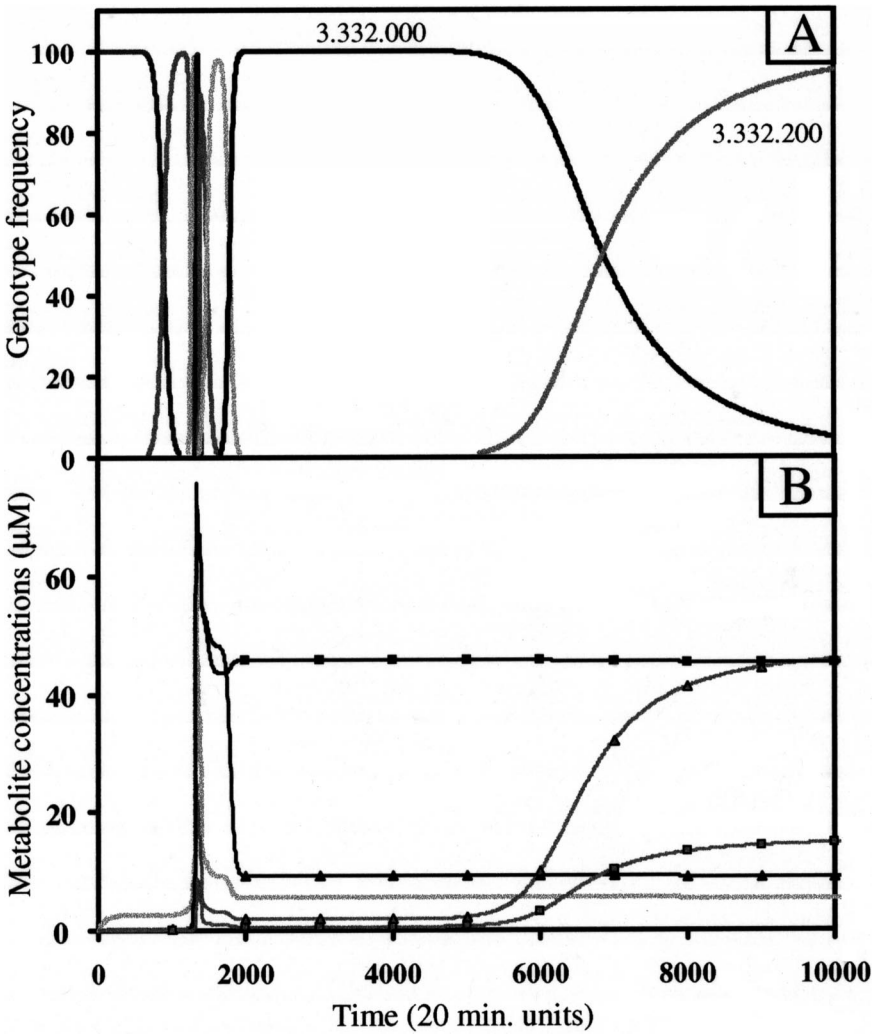

FIG. 6. Evolution of genotypic composition and substrates concentrations. (A) Changes in the genotypic frequencies. Each curve represents one genotype. For clarity, we show only the genotypes with frequencies ≥1%. The succession of genotypes during the first 2000 units of time is rapid and some curves are not discernible. The six first successive genotypes were the following: 0.000.000, 3.000.000, 3.300.000, 3.320.000, 3.321.000 and 3.322.000, respectively. (B) Changes in the substrate concentrations, B (gray line), C_1 (black line with triangle), D_1 (black line with box), C_2 (gray line with triangle), and D_2 (gray line with box). A is not represented here; its concentration remained constant in the environment (=1 mM) due to precipitation. Both curves correspond to the same simulation as in Figure 5; the values of the parameters were the same.

invading a resident one. For example, after 4000 time units, genotype 3.332.000 was replaced by 3.332.200 (Fig. 6A). Furthermore, when a major genotype predominated in the population (e.g., genotype 3.332.200 in Fig. 6A), this clone always coexisted with some 20 other mutant genotypes present at very low frequencies (10^{-5}; data not shown).

Varying the intracellular concentration of A ($[A]_i$) or the duration of the catalytic phase (Δt) had no qualitative influence on the behavior of the model (data not shown). For further simulations, we chose $[A]_i = 100$ μM and $\Delta t = 20$ min as reference values. When the maximum enzymatic activity of a cell increased, so did the number of major jumps and the final mean enzymatic activity of the population (Fig. 7). However, the general behavior of the model remained the same (data not shown). Because we wanted to impose a cost on enzyme production, we chose a maximum enzymatic activity of 35 min^{-1} for further simulations. This value allowed a maximum of three highly efficient enzymes per genotype. Concerning the other parameters (basal death rate; generation time; equilibrium constants of the reactions, $K_{i,j}$; and initial and maximum population size), the model was globally robust to small variations of these parameters, as long as their values remained realistic (data not shown). Death rate and initial population size had to be, respectively, small and high enough (<0.1 and $>5 \times 10^7$) to prevent total extinction of the population before it could adapt.

Influence of Resource Availability

The polymorphism within the population was affected by resource availability, J_A, in terms of genotype number and composition. The mean number of genotypes in an evolved population (no additional evolution detected, 50,000 units of time) was negatively correlated with resource availability (20

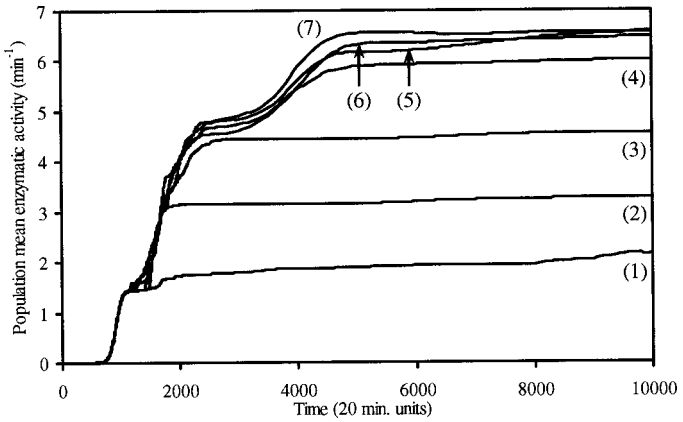

FIG. 7. Influence of maximum total enzymatic activity on the evolution of mean enzymatic activity. Ten simulations were run for different values of maximum total enzymatic activity. Each curve represents the mean of the 10 simulations. The values of maximum total enzymatic activity were (1) 15, (2) 25, (3) 35, (4) 45, (5) 55, (6) 65, and (7) 75 min^{-1}. Except for maximum activity, the values of the parameters were as in Figure 5.

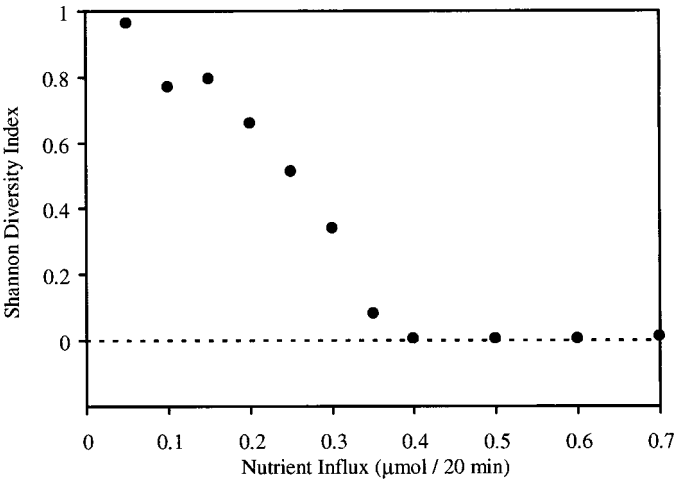

FIG. 8. Genotypic diversity and competition for food. The Shannon diversity index (Shannon and Weaver 1963; $= -\Sigma\ p_i \ln[p_i]$), calculated in an evolved population, after 50,000 units of time, is plotted against nutrient influx. Each dot represents the mean of 100 simulations. Except for J_A, the values of the parameters were as in Figure 5.

genotypes under 0.5 μmol/20 min vs. 60 genotypes under 0.05 μmol/20 min). This resulted in an increase of Shannon diversity index (Shannon and Weaver 1963) under low nutrient conditions (Fig. 8). The difference was still present and even greater when observed during the transitory phase (40 genotypes under 0.5 μmol/20 min vs. 160 genotypes under 0.05 μmol/20 min, after 10,000 units of time; data not shown).

When the influx of *A* was high (Fig. 9A), the population essentially experienced a succession of single genotypes, which, in the long term, ended in a monomorphic situation—a situation where a major genotype coexisted with rare mutants (frequency 10^{-5}). The final major genotype was characterized by its distribution of enzyme activities on the metabolic pathway: The three enzymes with highest activities (10 min^{-1}) were always located on branch 0 (A → B) and on the first two reactions of one branch (e.g., 3.332.221; Fig. 9A). These genotypes were called ''first (or second) branch-specific'' genotypes.

When the influx of *A* was decreased, stable polymorphic situations were frequently observed (Figs. 9B, C). The branch-specific genotypes were still present, but they possibly interacted with two other kinds of genotypes. Under intermediate values of nutrient availability, genotypes that distributed their highest activities on both branches sometimes appeared (3.321.321, Fig. 9B). We called these genotypes ''both branches users.'' Finally, under low nutrient influx, the final population was always trimorphic: The third kind of genotype was characterized by a high activity for one of the final reactions of the pathway (3.323.202, Fig. 9C). These genotypes were called ''last compound users.''

Frequency-Dependent Interactions and Competing Interactions

To detect possible frequency-dependent interactions between the three kinds of genotypes that arose during the simulations, their energy production was calculated in populations with various genotypic compositions and under various competitive situations: A population composed of fixed frequencies of the three genotypes 3.332.202, 3.321.321, and 3.323.202 (the main coexisting genotypes in Fig. 9) was created. Allowing no mutation or division, we let this population attain metabolic equilibrium (1000 generations) and then calculated the energy production of the three kinds of genotypes, using equation (10) (Fig. 10). For each graph, the frequency, *F*, of 3.323.202, a last compound user, was kept constant and we chose this genotype as a reference to calculate the relative fitness of the two remaining genotypes. We thus defined the fitness of a genotype as the ratio of its energy production on the energy production of genotype 3.323.202 ($W_g = E_g/E_{3.323.202}$). The fitness of the two other genotypes (3.332.202 and 3.321.321) was estimated as a function of their frequency, under various conditions of nutrient competition, and with various frequencies of genotype 3.323.202.

These calculations showed that the energy production of a genotype is strongly dependent on its frequency in the population and on the competition intensity (Fig. 10). The relative fitness of the three genotypes was always negatively correlated to their frequency. For example, the fitness of genotype 3.323.202 was high when its frequency was low (Fig. 10A) and decreased when its frequency increased (Fig. 10B, C). Moreover, relative fitness also depended on competitive conditions: Genotype 3.323.202 had a high fitness only under highly competitive conditions (Fig. 10A). The invasion of a genotype being possible only when its fitness is higher than the fitness of the competing genotypes, 3.323.202 could only invade a population when the nutrient influx was low ($J_A = 0.05$), and its equilibrium frequency was around 0.3, as shown by the intersection of the three fitness curves in Figure 10B.

DISCUSSION

The aim of this work was to use available knowledge on bacterial metabolism to model, as realistically as possible,

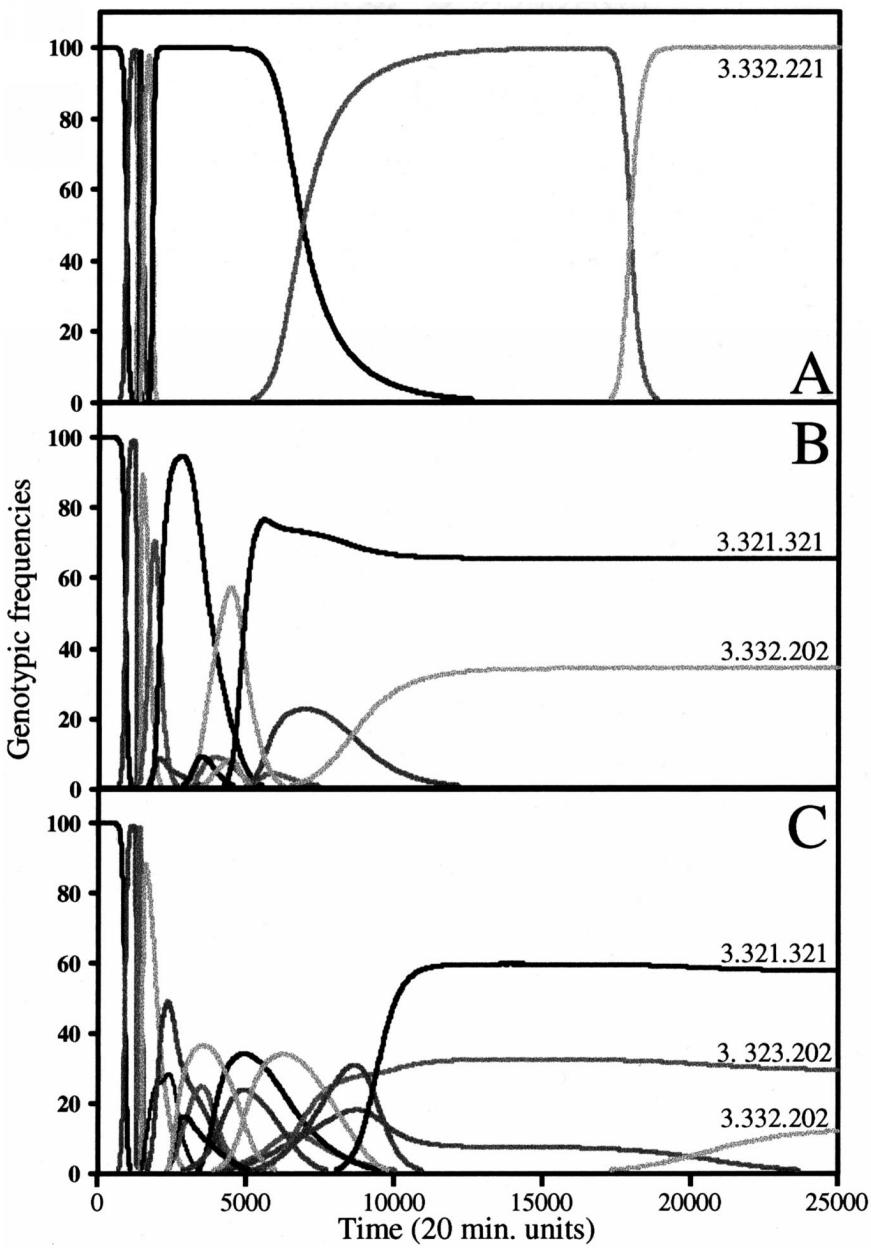

FIG. 9. Genotypic succession in various situations of nutrient competition. We ran the same simulation (same seed) for different values of nutrient influx and we followed the succession of genotypes in the population. The nutrient influx was: (A) 0.5, (B) 0.1, and (C) 0.05 μmol/20 min, and the other parameters were as in Figure 5.

the evolution of a bacterial population. In particular, we wanted to account for the experimental observations of stable polymorphisms in bacterial populations (Levin 1972; Rosenzweig et al. 1994; Rozen and Lenski 2000) without making any a priori assumptions on the potential mechanisms maintaining this polymorphism.

Realistic Evolution of the Modeled Population

We observed stepwise evolution (Fig. 5) of mean enzyme activity, which was also experimentally observed by Elena et al. (1996) studying the evolution of mean cell size. These authors suggested that the increase in cell size (and thus in fitness) could be due to a more rapid uptake of glucose or to a more efficient catabolism, i.e., to a change in protein activity. In our model, the stepwise evolution corresponded to the fixation of beneficial mutations, i.e., to the successive replacements of genotypes, as shown by the strong correlation between steps of mean activity and time of appearance of new genotypes (Figs. 5, 6). The similarity of our results and experimental observations (Elena et al. 1996) thus indicated that a model with discrete effects of mutations on enzymatic activities was appropriate to describe the evolution of quantitative traits related to bacterial metabolism.

The metabolic model constrained the sequence of fixation

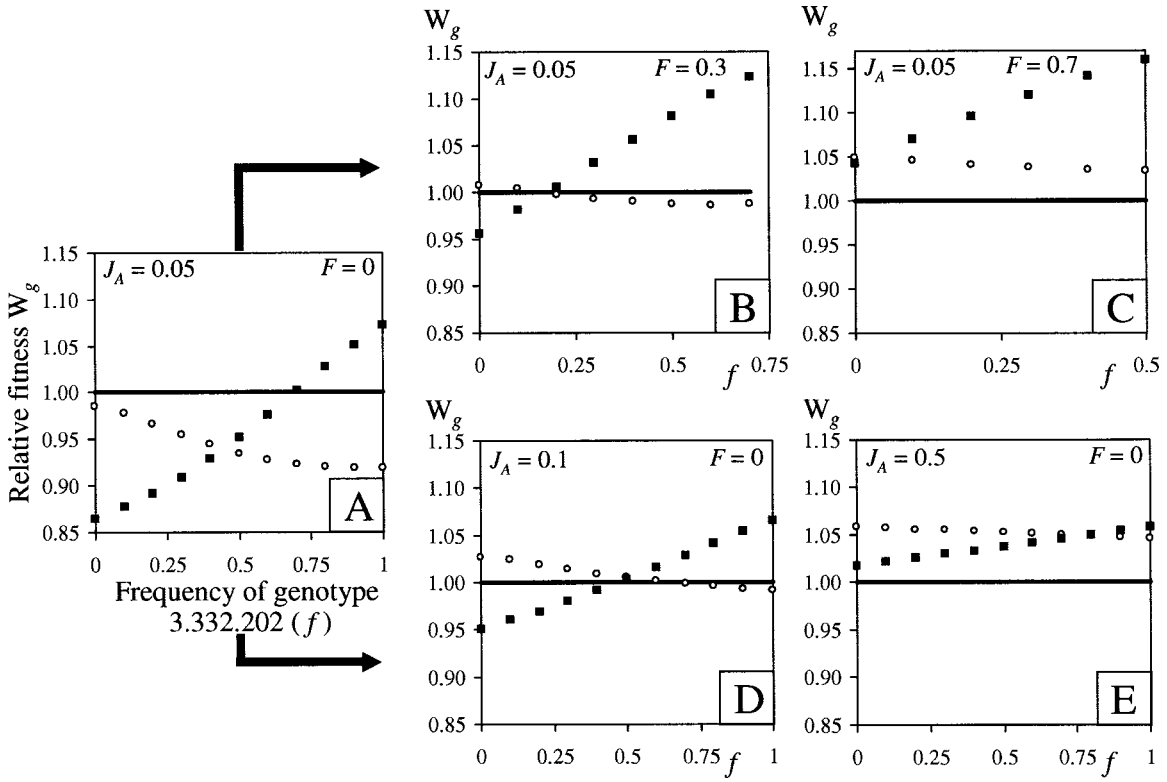

FIG. 10. Frequency dependent fitness in various conditions of nutrient competition. The fitness of three genotypes (3.332.202 [circle], 3.321.321 [box], and 3.323.202 [line]) was estimated in various conditions of genotypic frequencies (A → C) and in various conditions of nutrient competition (A, D, E). The fitness of a genotype g was $W_g = E_g/E_{3.323.202}$, which means that 3.323.202, a last compound user, had a reference fitness of one. For each graph, the frequency, F, of this last compound user genotype was kept constant, and we varied the frequency of the two remaining genotypes. The fitness of the three genotypes are plotted against the frequency, f, of genotype 3.332.202, for various values of F: (A) $F = 0$, (B) $F = 0.3$, and (C) $F = 0.7$, and for various values of nutrient influx: (A) $J_A = 0.05$, (D) $J_A = 0.1$, (E) $J_A = 0.5$ μM/20 min. The frequency of 3.321.321 was $(1 - f - F)$. A zero frequency meant that only one cell among 10^{10} was present in the population. Except for J_A, parameters values were as in Figure 5.

of beneficial mutations, which might provide explanations for the experimental observation of mutations being fixed independently of the magnitude of their effect on fitness (Elena et al. 1996). The growth rate of a genotype, defined as its energy production, depended on its biotic and abiotic environment: New genotypes could only invade when adequate metabolites were present in the environment, and these metabolites might be released by other genotypes. For example, at the beginning of a simulation, only genotypes having a high activity on the first reaction could invade, because *A* was the only available nutrient. These genotypes (e.g., 3.000.000, Fig. 6) released *B*, which in turn could be used by a mutant genotype catalyzing the degradation of *B* (in general 3.300.000 or 3.000.300, because all mutant genotypes were derived from 3.000.000, which invaded the population rapidly). The metabolic pathway was thus built progressively, from the first reactions to the last ones, which is consistent with theories of metabolic evolution of catabolic pathways (Gehring and Ikeo 1999). During the stepwise evolution observed by Elena et al. (1996) or Lenski and Travisano (1994), some mutations with small effects invaded before mutations with larger effects. This could be due to the same constraints on pathway assembly: The effect of a mutation could depend on the environmental conditions of the mutant genotype.

Mechanisms Maintaining Selected Polymorphisms

The evolving bacterial populations were always polymorphic with a minimum of 20 coexisting genotypes. Besides the transient polymorphism due to successive clonal replacements, we could discern two stable polymorphic situations.

Some genotypes were maintained by mutation/selection balance. When the population was monomorphic, in the sense that the frequency of the major genotype exceeded 99%, all possible mutants (21) deriving from the major genotype could be found. Although it could be important in terms of adaptive potential in a new environment, this polymorphism did not correspond to what is observed in experiments. The frequency of coexisting genotypes in the different experiments were always the order of several percent (Rosenzweig et al. 1994; Rozen and Lenski 2000), which was not the case in our simulations where the frequencies of mutant genotypes never exceeded 10^{-5} unless they were selected afterward. However, it is likely that mutation/selection balance acted in the experimental populations, but the resulting polymorphism could not be detected because of the very low frequencies of mutant genotypes.

Dimorphic or trimorphic stable situations, with genotypic frequencies larger than 10%, were observed under low-

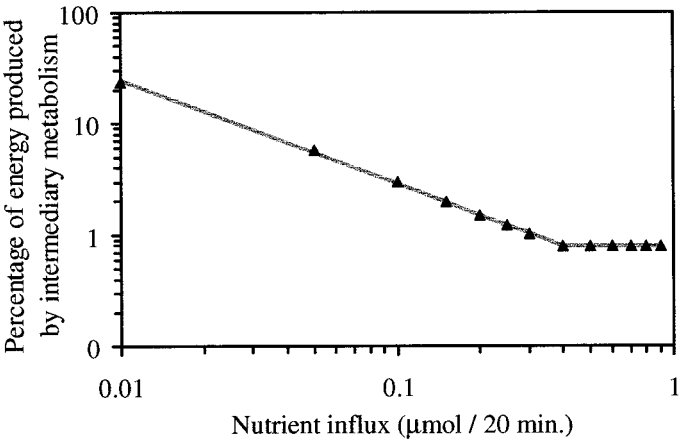

FIG. 11. Metabolism of intermediary products and competition for food. The simulations parameters are the same as in Figure 10. Knowing that the total amount of energy produced by a cell comes either from a constant flux through the metabolic pathway or from the consumption of intermediary products, the *y*-axis is (energy produced by the consumption of intermediary products)/(total amount of energy).

nutrient conditions. The population size being constant, these low-nutrient conditions resulted in competition for resources. The positive effect of competition on the polymorphism of the population confirmed the important role of metabolic interactions in the maintenance of a selected polymorphism, as proposed by Levin (1972), Turner et al. (1996), Elena and Lenski (1997), and Treves et al. (1998). The cross-feeding interactions in our model could be summarized as follows. Under noncompetitive conditions, *A* was always available; genotypes with a high metabolic flux through the pathway were the most efficient ones. When *A* started decreasing, genotypes that could grow on other organic compounds were favored. In fact, when competition increased, a larger part of the energy was produced through consumption of intermediary compounds of the metabolic pathway (Fig. 11). Thus, under strong competition (Fig. 9C), the metabolic interactions were schematically the following: 3.321.321 used *A* and *B* and released C_1 and C_2. C_1 could be consumed by 3.332.202, which in turn released D_1, on which 3.323.202 could grow. Of course, these strategies were not absolute; each genotype, using smaller levels of activities, could combine some of them (e.g., 3.332.202, a first branch-specific genotype, was also a last compound user on the second branch). In such a population, where metabolic activities were spread among clones, complete degradation of the energetic source and its derivatives was achieved by the whole community and not by a single genotype. This fact has to be taken into account if one is to use laboratory-evolved asexual bacteria as a means for environmental remediation (Liu and Suflita 1993).

The cross-feeding interactions of our model resulted in frequency-dependent selection (Fig. 10). When genotypes were rare, they had a greater amount of nutrients released by competing genotypes at their disposal. Frequency-dependent selection has already been shown in several experiments (Turner et al. 1996; Elena and Lenski 1997; Rozen and Lenski 2000), but the underlying mechanisms were not elucidated, although metabolism was often proposed. Our model suggests a possibly major role of metabolic interactions in the maintenance of stable selected polymorphisms through frequency-dependent selection.

The results described above (i.e., the existence of stable polymorphisms under competitive conditions) were somewhat independent of the hypotheses we chose for the model. First, the behavior of the model was globally robust to realistic changes in most parameters values. Second, as intuitively expected, a modification of the structure of the metabolic pathway implied major changes in genotype number and composition of the population. However, even with a simple linear metabolic pathway, polymorphic situations, with metabolic interactions between the genotypes, were still observed (data not shown). Finally, we also showed that the qualitative behavior of the model was not dependent on the constraints we imposed on enzyme production (Fig. 7). The level of polymorphism decreased when the constraints decreased, but polymorphic situations were always observed under competitive conditions, unless enzyme production was little or not constrained (all enzymes could reach maximum activity). This situation is nevertheless biologically unrealistic, because it has been largely demonstrated that enzyme production is limited in many organisms, including bacteria, due to volume limitation, energetic costs, or cytoplasm viscosity (see Brown 1991 and references therein). Our results are thus quantitatively dependent on a certain number of hypotheses, but they are robust, qualitatively speaking, regarding these hypotheses. This constancy of our results confirmed that the population structure we obtained was not an artifact and that our model might give a good description of what happened in experiments on bacterial polymorphism evolution.

Stable Selected Polymorphisms Were Only Maintained under Highly Competitive Conditions

Calculations showed that the minimum influx of *A* required to sustain the growth of a whole highly efficient population (10^{10} cells; e.g., genotype 3.332.202), was approximately 4 μM/20 min. Under this threshold value, there was competition for the resource. This competition for food was a necessary condition for the emergence of a stable polymorphism; simulations showed that the populations always remained monomorphic (one major genotype) under noncompetitive conditions (Fig. 8). There is no discrepancy between the theoretical need for competition and the experimental observations. In the different experimental approaches, the effect of competition was not studied, but populations were always grown in a nutrient-limited medium, implying a high level of competition (Levin 1972; Turner et al. 1996; Elena and Lenski 1997; Treves et al. 1998). To test this important effect of nutrient competition on polymorphism maintenance, additional experiments would be needed. For example, the addition of an excess of glucose in a polymorphic population of constant size should result in the disappearance of one or several genotypes.

The effect of competition on the level of polymorphism in bacterial populations was progressive. We obtained a positive relationship between the strength of competition (ex-

pressed as the influx of nutrient available for 10^{10} cells) and the level of polymorphism in the model bacterial populations (Fig. 8): The higher the competition, the higher the transient and stable selected polymorphisms in the population. We explained this pattern by the rarefaction of the main resource (*A*) and the emergence of new genotypes playing alternative strategies (consumption of intermediary metabolites). This quantitative influence of competition on the genetic diversity of populations has already been experimentally explored on *Pseudomonas fluorescens* in a laboratory microcosm (Kassen et al. 2000). In this study, a positive relationship between competitive strength and polymorphism was observed, but beyond a limit value of competition, the relationship is inverted: Diversity peaked at intermediary nutrient concentrations. This result was consistent with the predictions of a modified Levene's (1953) model for the maintenance of diversity in a heterogeneous environment (Kassen et al. 2000). Similarly, Turner et al. (1996) observed that polymorphism in an *E. coli* population could not be maintained if the level of nutrient was too low. This trend did not appear in our simulations, because under low nutrient concentrations (<0.05 μmol/20 min), the discreteness in time was no longer a pertinent simplification.

The coexistence of three different genotypes using apparently the same single resource in a temporally and spatially homogeneous environment (Fig. 9) does not fit the predictions of the competitive exclusion principle, which states that no more species can coexist than the number of limiting resources (Hardin 1960). However, a definition of resource needs to be specified. In our case, one can consider that the number of resources equals the number of metabolites present in the growing medium. Alternatively, we may deduce from the competitive exclusion principle that three resources were available because three genotypes coexisted at equilibrium. Whatever the choice, we are left with a semantic problem, as stated previously by Levin (1972), and the principle of competitive exclusion might not be a relevant approach to diversity maintenance in this biochemical and molecular context.

Acknowledgments

We thank C. Lavigne, J. Shykoff, and E. Lacey for careful reading of the manuscript and helpful comments; F. Taddei, C. Dillmann, B. Bost, and G. Bell for insightful discussions about the model; and P. H. Gouyon for input on this work.

Literature Cited

Alexander, M. 1981. Biodegradation of chemicals of environmental concern. Science 211:132–138.

Blattner, F. R., G. Plunkett III, C. A. Bloch, N. T. Perna, V. Burland, M. Riley, J. Collado-Vides, J. D. Glasner, C. K. Rode, G. F. Mayhew, J. Gregor, N. W. Davis, H. A. Kirkpatrick, M. A. Goeden, D. J. Rose, B. Mau, and Y. Shao. 1997. The complete genome sequence of *Escherichia coli* K-12. Science 277: 1453–1474.

Brown, G. C. 1991. Total cell protein concentration as an evolutionary constraint on the metabolic control distribution in cells. J. Theor. Biol. 153:195–204.

Dean, M. A., D. E. Dykhuizen, and D. L. Hartl. 1986. Fitness as a function of β galactosidase activity in *Escherichia coli*. Genet. Res. 48:1–8.

Dong, H., L. Nilsson, and C. Kurland. 1995. Gratuitous overexpression of genes in *Escherichia coli* leads to growth inhibition and ribosome destruction. J. Bacteriol. 177:1497–1504.

Drake, J. W. 1991. A constant rate of spontaneous mutation in DNA-based microbes. Proc. Natl. Acad. Sci. USA 88:7160–7164.

Dykhuizen, D. E., and M. A. Dean. 1990. Enzyme activity and fitness: evolution in solution. Trends Ecol. Evol. 5:257–262.

Elena, S. F., and R. E. Lenski. 1997. Long-term experimental evolution in *Escherichia coli*. VII. Mechanisms maintaining genetic variability within populations. Evolution 51:1059–1067.

Elena, S. F., V. S. Cooper, and R. E. Lenski. 1996. Punctuated evolution caused by selection of rare beneficial mutations. Science 272:1802–1804.

Ferenci, T. 1996. Adaptation to life at micromolar levels: the regulation of *Escherichia coli* glucose transport by endoinduction and cAMP. FEMS Microbiol. Rev. 18:301–317.

Gehring, W. J., and K. Ikeo. 1999. Pax 6: mastering eye morphogenesis and eye evolution. Trends Genet. 15:371–377.

Hardin, G. 1960. The competitive exclusion principle. Science 131: 1292–1297.

Hastings, I. M. 1992. The population genetics of alleles affecting enzyme activity. J. Theor. Biol. 157:305–316.

Kacser, H., and R. Beeby. 1984. Evolution of catalytic proteins: on the origin of enzymes by means of natural selection. J. Mol. Evol. 20:38–51.

Karp, P., M. Riley, S. Paley, A. Pellegrini-Toole, and M. Krummenacker. 1999. EcoCyc: electronic encyclopedia of *E. coli* genes and metabolism. Nucleic Acids Res. 27:55.

Kassen, R., A. Buckling, G. Bell, and P. B. Rainey. 2000. Diversity peaks at intermediate productivity in a laboratory microcosm. Nature 406:508–512.

Keightley, P. D., and H. Kacser. 1987. Dominance, pleiotropy and metabolic structure. Genetics 117:319–329.

Koch, A. L. 1983. The protein burden of lac operon products. J. Mol. Evol. 19:455–462.

Leahy, J. G., and R. R. Colwell. 1990. Microbial degradation of hydrocarbons in the environment. Microbiol. Rev. 54:305–315.

Lee, M. D., J. M. Odom, and R. J. Buchanan Jr. 1998. New perspectives on microbial dehalogenation of chlorinated solvents: insights from the field. Annu. Rev. Microbiol. 52:423–452.

Lenski, R. E., and M. Travisano. 1994. Dynamics of adaptation and diversification: a 10,000-generation experiment with bacterial populations. Proc. Natl. Acad. Sci. USA 91:6808–6814.

Levene, H. 1953. Genetic equilibrium when more than one ecological niche is available. Am. Nat. 87:331–333.

Levin, B. R. 1972. Coexistence of two asexual strains on a single resource. Science 175:1272–1274.

———. 1988. Frequency-dependant selection in bacterial populations. Philos. Trans. R. Soc. Lond. B 319:459–472.

Liu, S., and J. M. Suflita. 1993. Ecology and evolution of microbial populations for bioremediation. Trends Biotechnol. 11:344–352.

Macaskie, L. E., P. Yong, T. C. Doyle, M. G. Roig, M. Diaz, and T. Manzano. 1997. Bioremediation of uranium-bearing wastewater: biochemical and chemical factors influencing bioprocess application. Biotechnol. Bioeng. 53:100–109.

Prescott, L. M., J. P. Harley, and D. A. Klein. 1996. Microbiology. 3rd ed. W. C. Brown, Dubuque, IA.

Rainey, P. B., and M. Travisano. 1998. Adaptive radiation in a heterogeneous environment. Nature 394:69–72.

Rainey, P. B., A. Buckling, R. Kassen, and M. Travisano. 2000. The emergence and maintenance of diversity: insights from experimental bacterial populations. Trends Ecol. Evol. 15: 234–247.

Rosenzweig, R. F., R. R. Sharp, D. S. Treves, and J. Adams. 1994. Microbial evolution in a simple unstructured environment: genetic differentiation in *Escherichia coli*. Genetics 137:903–917.

Rozen, D. E., and R. E. Lenski. 2000. Long term experimental evolution in *Escherichia coli*. VIII. Dynamics of a balanced polymorphism. Am. Nat. 155:24–35.

Savageau, M. A. 1983. *Escherichia coli* habitats, cell types and molecular mechanisms of gene control. Am. Nat. 122:732–744.
Senez, J. C. 1962. Some considerations on the energetics of bacterial growth. Bacteriol. Rev. 26:95–107.
Shannon, C. E., and W. Weaver. 1963. The mathematical theory of communication. Univ. of Illinois Press, Urbana, IL.
Stewart, F. M., and B. R. Levin. 1973. Partitioning of resources and the outcome of interspecific competition: a model and some general considerations. Am. Nat. 107:171–198.
Tenaillon, O., B. Toupance, H. Le Nagard, F. Taddei, and B. Godelle. 1999. Mutators, population size, adaptive landscape and the adaptation of asexual populations of bacteria. Genetics 152: 485–493.
Treves, D. S., S. Manning, and J. Adams. 1998. Repeated evolution of an acetate-crossfeeding polymorphism in long-term populations of *Escherichia coli*. Mol. Biol. Evol. 15:789–797.
Turner, P. E., V. Souza, and R. E. Lenski. 1996. Tests of ecological mechanisms promoting the stable coexistence of two bacterial genotypes. Ecology 77:2119–2129.

Corresponding Editor: H. Ochman

Appendix

Steady-State Concentrations of Metabolites in the Branched Pathway

In the branched pathway (Fig. 1), at steady state, the velocities of the reactions are $J_0 = (1/a_0)\{[A] - [B]_{SS}/K_{0,1}\}$, $J_1 = ([B]_{SS}/a_1)$, and $J_2 = ([B]_{SS}/a_2)$ (see text for detailed calculations). Knowing that

$$J_0 = e_{0,1}([A] - [B]_{SS}/Ke_{0,1}), \quad \text{(A1)}$$

$$J_1 = e_{1,1}([B]_{SS} - [C_1]_{SS}/Ke_{1,1}) = e_{1,2}([C_1]_{SS} - [D_1]_{SS}/Ke_{1,2}), \quad \text{(A2)}$$

and

$$J_2 = e_{2,1}([B]_{SS} - [C_2]_{SS}/Ke_{2,1}) = e_{2,2}([C_2]_{SS} - [D_2]_{SS}/Ke_{2,2}), \quad \text{(A3)}$$

we have:

$$[C_1]_{SS} = Ke_{1,1}[B]_{SS}[1 - (1/e_{1,1}a_1)], \quad \text{(A4)}$$

$$[C_2]_{SS} = Ke_{2,1}[B]_{SS}[1 - (1/e_{2,1}a_2)], \quad \text{(A5)}$$

$$[D_1]_{SS} = Ke_{1,2}[B]_{SS}\{Ke_{1,1}[1 - (1/e_{1,1}a_1)] - 1/e_{1,2}a_1\}, \quad \text{and} \quad \text{(A6)}$$

$$[D_2]_{SS} = Ke_{2,2}[B]_{SS}\{Ke_{2,1}[1 - (1/e_{2,1}a_2)] - 1/e_{2,2}a_2\}. \quad \text{(A7)}$$